Available online at www.sciencedirect.com

ScienceDirect

Current Opinion in Chemical Biology

Recent developments in spontaneous Raman imaging of living biological cells

Bianca Durrant[1,3], Matthew Trappett[1,3], Dustin Shipp[1] and Ioan Notingher[2]

Raman spectroscopy is a non-invasive optical technique for measuring chemical information from samples including biological cells. With its high sensitivity and compatibility with *in vitro* samples, Raman spectroscopy is increasing in popularity as a tool for acquiring chemical images of cellular samples in fields including parasitology, pharmacology, and oncology. This review describes emerging technologies that are improving the speed, resolution, and impact of Raman imaging techniques. Topics include novel instrumentation for data acquisition and improvements on techniques for displaying hyperspectral data as images.

Addresses
[1] Department of Physics, Utah Valley University, 800 West University Parkway, Orem, UT 84058, United States
[2] School of Physics and Astronomy, University of Nottingham, University Park, Nottingham NG7 2RD, United Kingdom

Corresponding author:
Notingher, Ioan (ioan.notingher@nottingham.ac.uk)
[3] These authors contributed equally to this work.

Current Opinion in Chemical Biology 2019, **51**:138–145

This review comes from a themed issue on **Molecular imaging**

Edited by **Philipp Kukura** and **Sua Myong**

For a complete overview see the Issue and the Editorial

Available online 22nd July 2019

https://doi.org/10.1016/j.cbpa.2019.06.004

Introduction

Raman spectroscopy is a sensitive technique using light scattering to probe the chemical composition of a sample. Various molecular vibrations in the sample cause unique wavelength shifts allowing researchers to measure the relative concentrations of chemical components, for example, lipids, proteins and DNA (see Figure 1) [1,2]. Absolute concentrations can also be obtained with appropriate calibration models [3,4]. Raman spectroscopy is a popular technique for chemical imaging microscopic biological samples as it is non-invasive, non-destructive, and compatible with aqueous samples [5]. Raman spectroscopy has been shown to detect slight chemical changes in tumor cells [6,7], differentiating stem cells [8,9], infected red blood cells [10], and cells with mitochondrial dysfunction [11].

However, significant concerns in Raman spectroscopy are the low signal and long acquisition times compared to other techniques, requiring 0.5–10 seconds per spectrum or 2–3 hours per 100×100 pixel image [12]. Consequently, a great deal of effort has been exerted into developing techniques to improve the imaging speed of Raman spectroscopy.

This review describes recent progress addressing the long acquisition time and other obstacles in Raman hyperspectral imaging. We will first describe various techniques – including emerging technologies – for acquiring spontaneous Raman spectra for the creation of hyperspectral images of live cells. We will then describe basic and developing methods for displaying these spectra as images.

Data acquisition techniques in spontaneous Raman scattering

Scanning techniques

Creating a hyperspectral Raman image requires the acquisition of several Raman spectra at various locations. Most spectra for Raman imaging continue to be acquired using point scanning, as this requires no technical upgrades over the basic Raman microscope. While relatively slow, this strategy has demonstrated sufficient time resolution to visualize uptake and localization of diatomite nanoparticles (see Figure 2(a)) [13], parasite incorporation of host cell proteins [3], and aggregation of different forms of $CaCO_3$ [14].

Raman imaging time can be decreased by using multiple rows of a CCD sensor to acquire multiple Raman spectra simultaneously. Line-scanning acquires spectra from a line of points and can be on the order of 20 times faster, albeit at the expense of depth sensitivity and confocality [15]. Line scanning is particularly useful when speed is a major concern, for example when imaging of large tissue samples [16]. Line scanning has also been used to acquire images of cells being fixed by various methods (see Figure 2(b)) [17] and cells growing neurites (see Figure 2(c)) [18]. Line scanning reduced the image acquisition time to provide sufficient temporal resolution to resolve these processes.

Figure 1

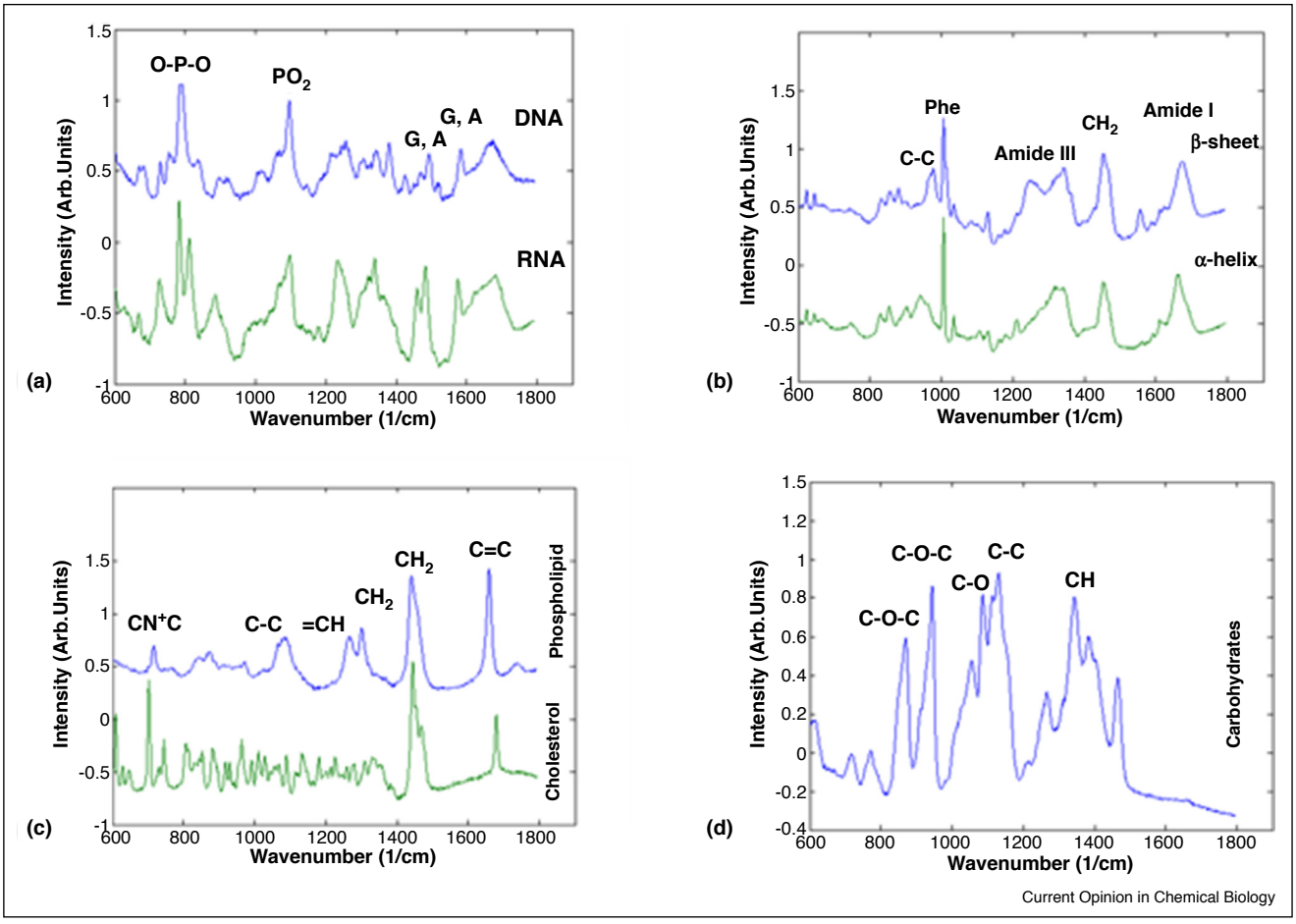

Raman spectra of common molecular classes in biological specimens. **(a)** Nucleic acid spectra include bands from the phosphate backbone and nucleotides. **(b)** Spectra from proteins are dominated by the Amide backbone and a strong contribution from phenylalanine. **(c)** The hydrocarbon chains of lipids contribute several strong Raman bands. **(d)** The carbon–oxygen bonds produce multiple unique bands in carbohydrate spectra. Reproduced from Ref. [1].

Multifocus Raman imaging is similar to line scanning, but arranges excitation beams *ad hoc* throughout the field of view, adding more versatility and real-time adaptability. This technique was used to image parasites with improved temporal resolution over point scanning, while maintaining a similar level of depth sectioning, as shown in Figure 2(d) [15].

In contrast, selective scanning exploits spatial correlation within samples to reduce the number of spectra required and can significantly decrease overall acquisition times. Multiple algorithms have been developed using feedback from early Raman spectra to optimize the locations for future Raman spectra. For example, Zhang *et al.* developed an dynamic sampling algorithm that used classification by a support vector machine (SVM) to guide subsequent measurements, reducing the time for imaging of mixed bisulfate forms by a factor of six without significant loss of classification accuracy or spatial resolution (see Figure 2(e)) [19•]. Another technique developed by Rowlands *et al.* interpolates spatial features based on surrounding spectra, allowing images to be reconstructed with 10–30 times fewer Raman measurements [20,21]. One can also reduce the number of Raman spectra necessary for an image by incorporating spatial information from another source. For example, auto-fluorescence images were used to guide Raman measurements during breast [22] and skin cancer surgeries [23], reducing the time to image large tissue samples from several hours to minutes.

Imaging with time-resolved Raman spectroscopy

In some samples, high levels of fluorescent background can be orders of magnitude stronger than the Raman signal, causing the Raman signal to be lost in noise. Time-resolved Raman spectroscopy employs time-gating

Figure 2

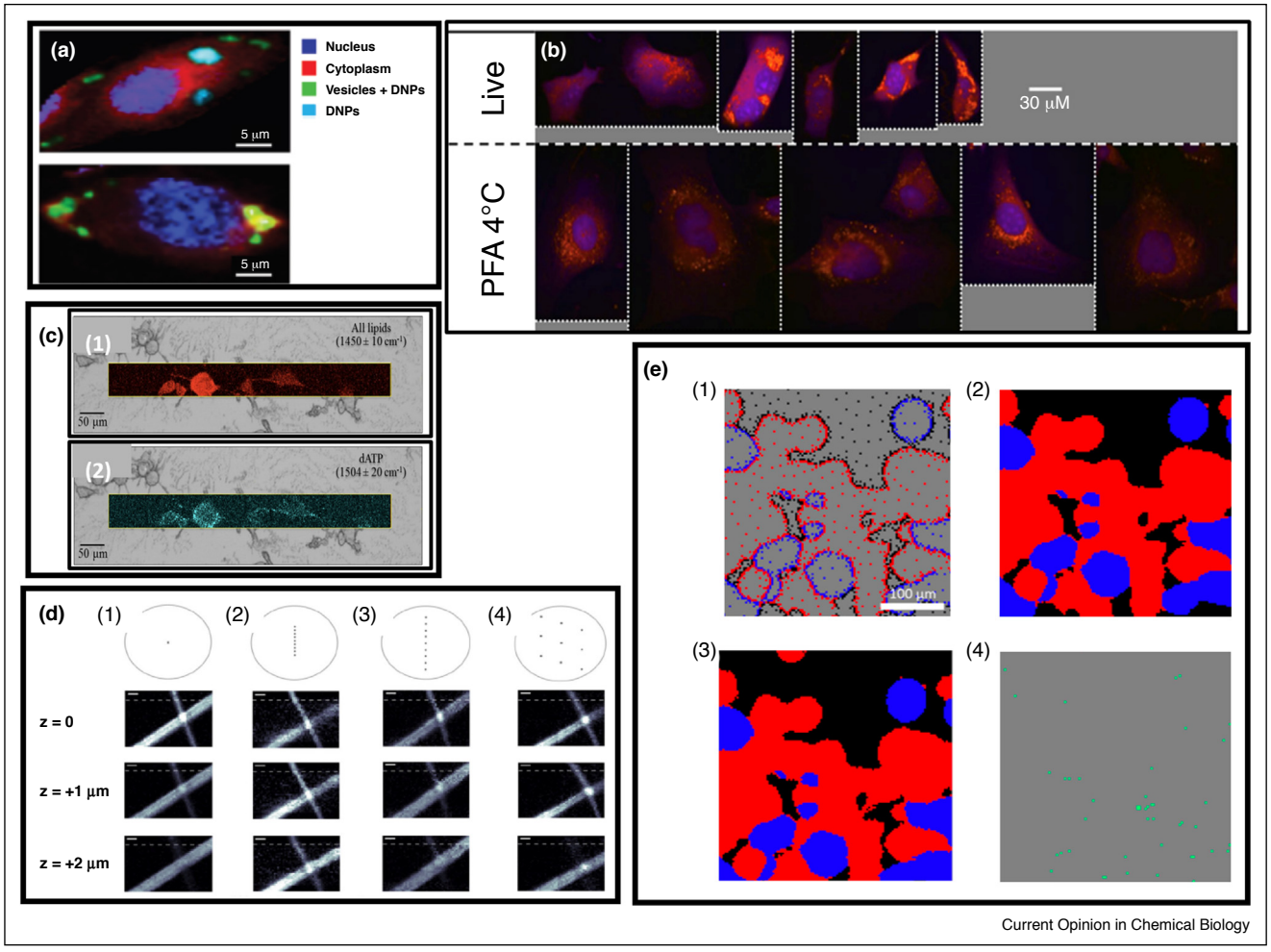

Examples of Raman images obtained by various scanning methods. **(a)** Raman images of cancer cells six and eighteen hours after incubation with diatomite. Images were obtained by point scanning (modified from Managó *et al.* [13]). **(b)** Line scanning Raman imaging of live mouse embryo cells to compare spectral profiles of fixations methods. PCA images are overlaid for each image. PC1 (blue) contains spectral components assigned to protein and lipid. PC2 (negative score in red) contains negative bands assigned to nucleic acids (modified from Hobro *et al.* [17]). **(c)** Line-scanned Raman images of (**1**) elementary phospholipids and (**2**) deoxy-nucleo-triphosphates were used to observe in a living neuron cell during neuronal separation and networking (modified from Pezzotti *et al.* [18]). **(d)** Images of overlaid diphenylalanine microtubes at different focal planes. Images were acquired using multifocus Raman to demonstrate the depth resolution of various configuration (modified from Liao *et al.* [15]). **(e)** Classification images of bisulfate forms. The image in (2) was generated using a complete raster scan. The image in (3) was generated using only the measurement locations (shown in (1)) chosen by the dynamic sampling algorithm. Green dots in (4) identify misclassified locations in (3) (modified from Zhang *et al.* [19•]).

to detect Raman scattered photons, which are emitted femtoseconds after irradiation, and reject fluorescence, which occurs picoseconds after. While effective, most time-resolved Raman techniques require scanning across the spectrum, slowing the acquisition. A method by Corden *et al.* uses a combination of prisms and a digital micromirror device (DMD) to combine multiple Raman bands on a time-sensitive detector. Raman bands can be chosen based on *a priori* sample information, eliminating the need for spectral scanning. Faster time-resolved Raman spectroscopy can acquire images like those in Figure 3(a) from highly fluorescent specimens which otherwise might have been difficult or time consuming to denoise [24•].

Raman labeling

Instead of targeting specific molecules like fluorescent labels, most Raman spectroscopy identifies slight changes in the relative concentrations of molecular classes (e.g. proteins, lipids, nucleic acids, etc., see Figure 1). Still, some specialized techniques use Raman labels to track specific molecules. Both stable isotope and alkyne labels

Figure 3

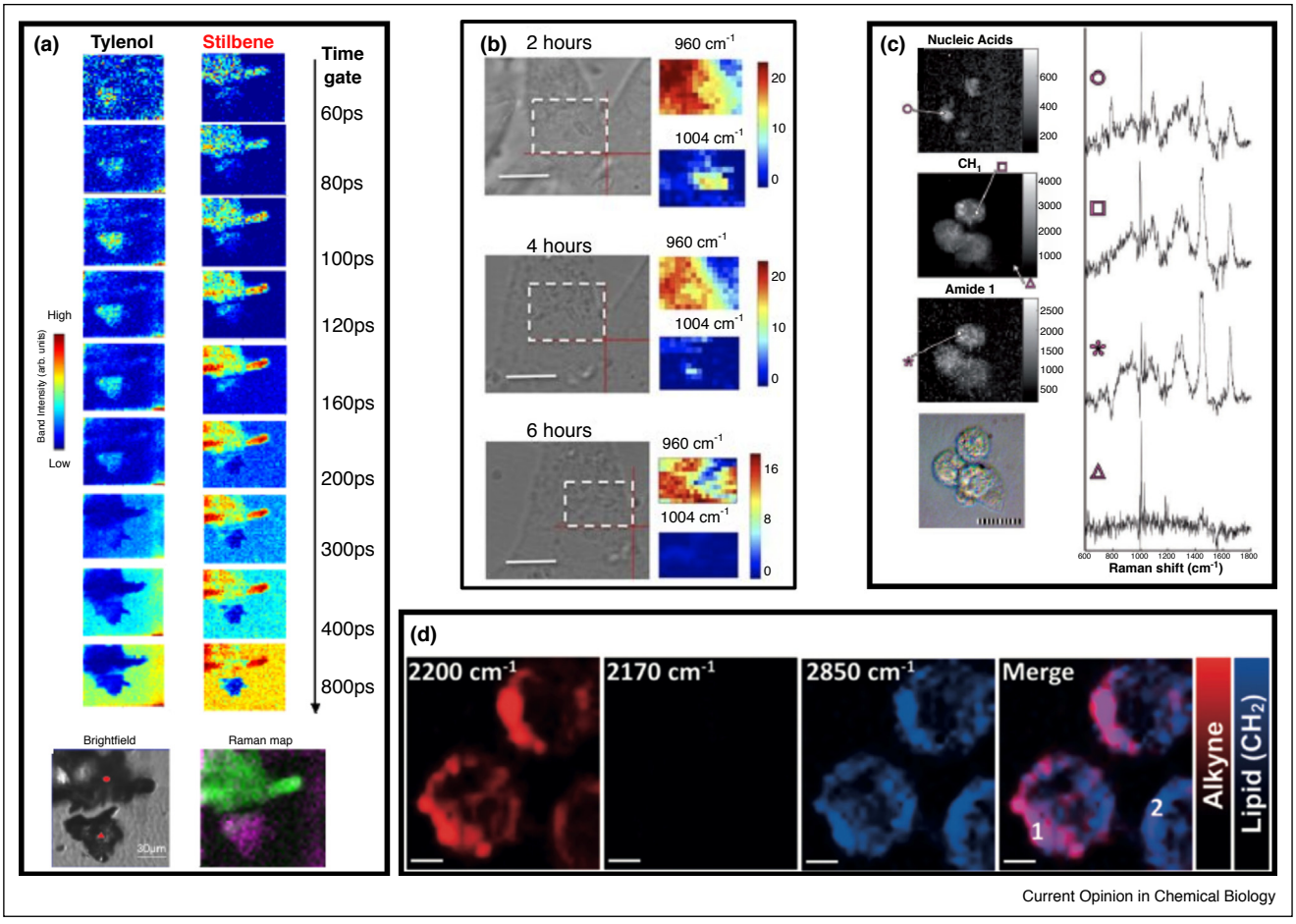

(a) Time-gated Raman measurements of a mixture of Tylenol and Stilbene in the presence of fluorescent dye. The appropriate time-gate measures Raman scattered photons while rejecting fluorescence (modified from Corden *et al.* [24•]). **(b)** Time-lapsed Raman images of amino acid transfer from host cell to parasite. The parasite and host are differentiated using stable isotope labeling (modified from Naemat *et al.* [3]). **(c)** Raman images of cells on a polystyrene substrate. Despite the strong polystyrene signal, background subtraction can reveal biochemical components such as nucleic acids, lipids, and proteins (modified from Sinjab *et al.* [29•]). **(d)** Raman images of HeLa cells after uptake of alkyne-labeled polymer nanoparticles. The alkyne bond produces a unique Raman band at 2200 cm^{-1} (modified from Li *et al.* [27]).

provide a minimally invasive way to greatly increase the specificity of Raman images.

Stable isotope labels (e.g. deuterium, ^{13}C) can be incorporated into the sample's cells, usually by incubation in the cell growth media. Because the isotopes are slightly heavier, the molecules containing them have lower vibrational energies that can be detected by shifted Raman bands. Thus, the labeled molecules can be tracked within a single cell or during cell–cell transitions yet remains non-destructive [25]. Stable isotope labels have been used to track nutrient exchanges as a parasite infects a host cell, as shown in Figure 3(b) [3,26].

An alternative labeling method involves adding alkyne structures to the molecule of interest. Bands from alkyne vibrations appear in the quiet spectral region between 1800 and 2800 cm^{-1}. This allows the labeled molecule to be isolated from other molecules in the spectrum by enhancing the Raman signal for that molecule, expanding its use in imaging. For example, Li *et al.* used alkyne labels to monitor polymer uptake in cells, as shown in Figure 3(d) [27].

Techniques for data processing and analysis

Spectral processing for background removal

Traditionally, Raman spectroscopy has used cells cultured on substrates with low Raman signals (e.g. quartz, CaF_2, MgF_2) [28]. Recently, Sinjab *et al.* have demonstrated Raman imaging on polymer substrates (see Figure 3(c)) [29•], similar to those used in biomaterial research, drug screening, and toxicology. This application was made

possible by an algorithm that iteratively removed both autofluorescence and substrate-generated Raman signal while preserving Raman peaks originating from the sample.

Other unwanted signals can come from the sample itself. Most Raman spectroscopy studies remove non-Raman background from acquire spectra through polynomial subtraction [30]. However, Prats-Mateu *et al.* investigated three multivariate algorithms for decoupling the Raman signal of interest from other spectral components in plant cell walls [31]. They used these multivariate techniques to unmix the acquired Raman spectra into several chemical constituents, allowing them to be subtracted or studied individually. This study also explored the effects of baseline correction and other spectral pre-processing on Raman images, finding that the ideal combination of processing and multivariate algorithms depended on the sample under study. A detailed review on such pre-processing and post-processing algorithms was written by Byrne *et al.* [32].

Univariate Raman imaging

After acquiring a Raman imaging dataset with spatial and spectral information (x, y, and wavenumber, see Figure 4(a)), a variety of methods can be used to transform these data into a useable image. These techniques vary from direct display of band intensities to more advanced statistical methods.

The workhorse of generating images from Raman spectra continues to be univariate imaging. This technique displays the intensity of a particular Raman band at each location in the image, essentially visualizing the relative concentration of a particular molecule throughout the sample. As shown by Pezzotti *et al.* (see Figure 2(c)), univariate techniques can be used to generate images of the concentrations of general classes of molecules such as lipids or specific molecules such as deoxyadenosine triposphate (dATP) [18].

Univariate imaging is particularly useful when the target molecule is known *a priori*. Two examples are cyclopropane fatty acids (CFAs) in yeast studied by Kochan *et al.* [33] and $CaCO_3$ uptake and transformation observed by Abalymove *et al.* [14]. Each of these studies concentrated on the Raman signal of a single molecule within a complicated system to reveal changes in chemical distribution and composition.

Furthermore, the addition of labels with unique Raman bands can allow imaging specific to the labeled particle. This strategy was applied by Yildirim *et al.* using rhetinoic acid's unique Raman band at 1596 cm^{-1} to track nanoparticles, as shown in Figure 4(b) [34].

Multivariate Raman imaging

Multivariate techniques, in contrast, use multiple Raman bands simultaneously to display the molecular properties of the sample. Unsupervised techniques can be used to identify key spectral features without any *a priori* information. The most common unsupervised techniques are principal component analysis (PCA) and cluster analysis. PCA finds a set of linearly independent variables, called principal components (PCs), that capture the most variance in the dataset. PCA images are generated by plotting the PC scores at each pixel [7]. An example of this can be seen in Figure 4(c), which uses the PC correlated to lipid activity to reveal differences in cell structure between normal and tumor cells [35].

Cluster analysis identifies groups of similar spectra, assigning colors to each cluster to visualize spectrally similar regions. The average (or centroid) spectrum from each cluster can be analyzed to discover chemical trends within each cluster. For example, Perez-Guaita *et al.* employed cluster analysis to visualize the spatial distributions and spectral components of hemozoin from parasites infecting red blood cells (see Figure 4(d)) [10].

Raman studies have recently begun adopting other unsupervised methods. Managó *et al.* implemented multivariate curve resolution-alternating least square (MCR-ALS), an unsupervised technique that iteratively optimizes the spectra of assumed pure components at the concentrations of those components [13]. Kallepitis *et al.* used vertex component analysis (VCA) in their three dimensional rendering of cell images (see Figure 4(e)) [36••]. VCA assumes that pixels of pure chemical constituents are present in the image and calculates concentrations of these constituents in the other pixels. These and other multivariate techniques are applied and compared by Prats-Mateu *et al.* [31].

Classification-based Raman imaging

As hyperspectral Raman imaging becomes more common and classification models become faster and more sophisticated, the two have been combined to generate diagnostic images directly based on parameters of interest (e.g. cell type, diagnosis, etc.). Zhang *et al.* trained a support vector machine (SVM) to identify bisulfate forms. Combined with a spectral feedback algorithm for dynamic sampling of Raman measurement locations, classification images were extended to locations not directly measured (see Figure 2(e)) [19•]. Other studies chose Raman measurement locations based on fluorescence images. Image segmentation algorithms allowed diagnoses by linear discriminant analysis [22] or artificial neural networks [23] to be extended in images to regions beyond where spectra were acquired. In each of these cases, point-by-point classification by Raman spectroscopy was too slow for the application, but selective sampling could effectively apply the classifier to each pixel in the image.

Outlook and conclusions

Raman spectroscopy includes several techniques that can be used to obtain chemical images of cellular samples,

Figure 4

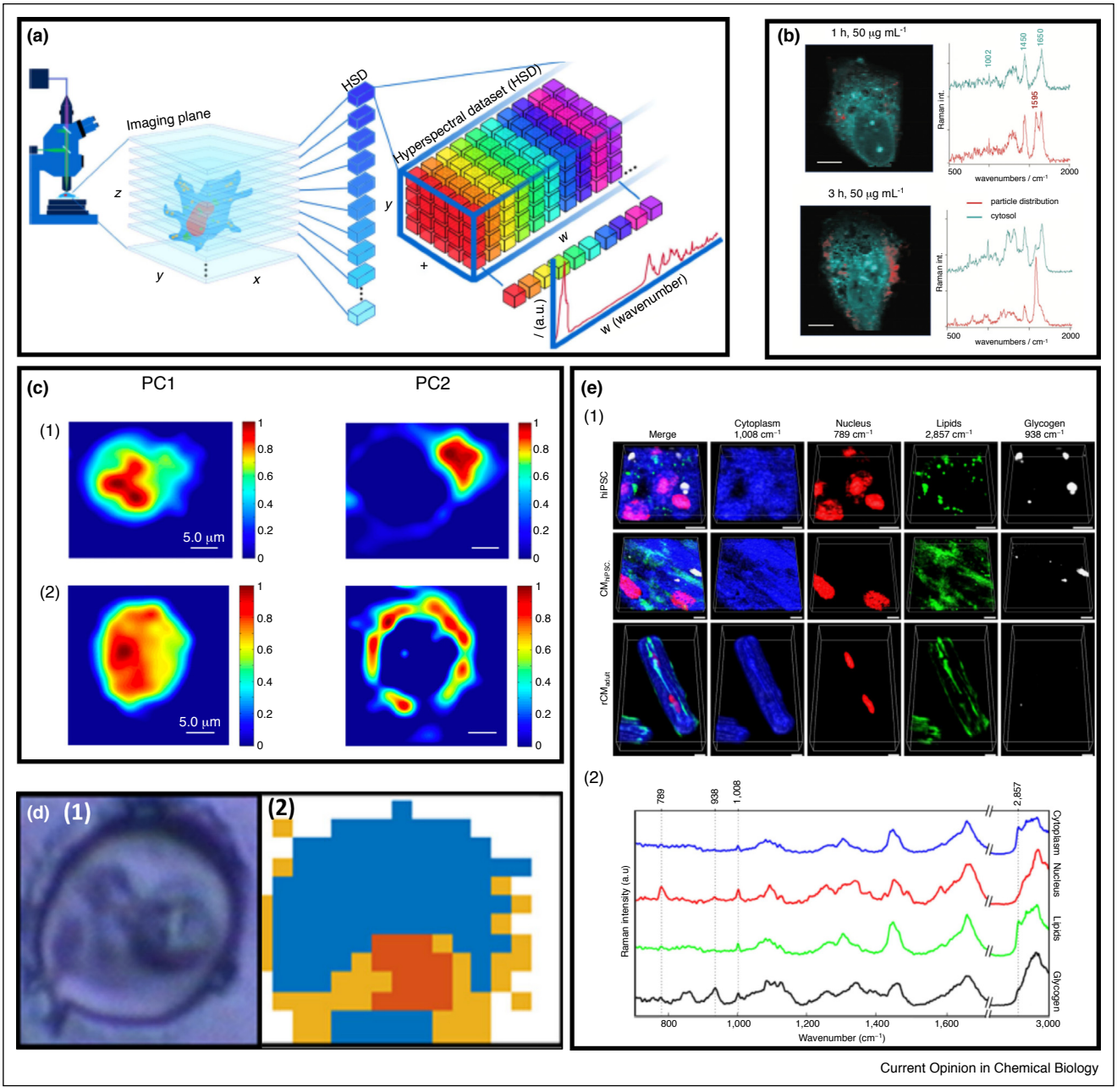

(a) Schematic of a hyperspectral dataset (sometimes called a hyperspectral data cube). Various algorithms exist to display this dataset as useful images (modified from Kallepitis *et al.* [36••]). **(b)** Raman images of LX-2 cells after incubation with nanoparticles. Nanoparticles were marked with rhetinoic acid for easy identification by the unique Raman band at 1596 cm^{-1} (modified from Yildirim *et al.* [34]). **(c)** Principal component analysis (PCA) images of (1) normal cells (PNT2) and (2) tumor cells (PC3-H2). The second principal component (PC2) reveals that in normal cells, lipid activity is concentrated whereas tumor cell lipid activity is distributed across the cell membrane (modified from Musto *et al.* [35]). **(d)** (1) Optical image and (2) Raman hyperspectral image of micrasterias. The Raman image was generated using unsupervised hierarchical cluster analysis. Clusters identify the location of a parasite infecting the cell (modified Perzer-Guaita *et al.* [13]). **(e)** Three-dimensional cell images produced by vertex component analysis to identify pure spectral components (modified from Kallepitis *et al.* [36••]).

particularly *in vitro*. While the low imaging speed has been the traditional weakness of this technique, Raman imaging offers some unique features including molecular specificity, non-invasiveness, and negligible sample preparation. Furthermore, advances in scanning methods are greatly improving the speed of acquiring Raman data. A variety of analysis methods are being developed to transform hyperspectral Raman data into more meaningful images.

These improvements along with high sensitivity and low sample preparation will enable Raman imaging to have significant impact in the analysis of infections, pharmaceuticals, and several other applications.

Conflict of interest statement

Nothing declared.

Acknowledgements

This work was supported by the Engineering and Physical Sciences Research Council [grant number EP/L025620/1, EP/M506588/1] and Utah Valley University Undergraduate Research Scholarly and Creative Activities (URSCA).

References and recommended reading

Papers of particular interest, published within the period of review, have been highlighted as:

- • of special interest
- •• of outstanding interest

1. Shipp DW, Sinjab F, Notingher I: **Raman spectroscopy: techniques and applications in the life sciences**. *Adv Opt Phot* 2017, **9**:315-427.
2. Cheng JX, Xie XS: **Vibrational spectroscopic imaging of living systems: an emerging platform for biology and medicine**. *Science* 2015, **350**:aaa8870.
3. Naemat A, Elsheikha HM, Boitor RA, Notingher I: **Tracing amino acid exchange during host-pathogen interaction by combined stable-isotope time-resolved Raman spectral imaging**. *Sci Rep* 2016, **6**:20811.
4. Boitor R, Sinjab F, Srohbuecker S, Sottile V, Notingher I: **Towards quantitative molecular mapping of cells by Raman microscopy: using AFM for decoupling molecular concentration and cell topography**. *Faraday Discuss* 2016, **187**:199-212.
5. Steward S, Priore RJ, Nelson MP, Treado PJ: **Raman imaging**. *Annu Rev Anal Chem* 2012, **5**:337-360.
6. Brauchle E, Schenke-Layland K: **Raman microspectroscopy for the development and screening of recombinant cell lines**. *Biotechnol J* 2017, **12**:1600412.
7. Jamieson LE, Harrison DJ, Campbell CJ: **Raman spectroscopy investigation of biochemical changes in tumour spheroids with ageing and after treatment with staurosporine**. *J Biophotonics* 2018:e201800201.
8. Pascut FC, Goh HT, Welch N, Buttery LD, Denning C, Notingher I: **Noninvasive enhanced detection and imaging of molecular markers in live cardiomyocytes derived from human embryonic stem cells**. *Biophys J* 2011, **100**:251-259.
9. Pascut FC, Kalra S, George V, Welch N, Denning C, Notingher I: **Non-invasive label-free monitoring the cardiac differentiation of human embryonic stem cells in-vitro by Raman spectroscopy**. *Biochim Biophys Acta Gen Subj* 2013, **1830**:3517-3524.
10. Perez-Guaita D, Kochan K, Martin M, Andrew DW, Heraud P, Richards JS, Wood BR: **Multimodal vibrational imaging of cells**. *Vib Spectrosc* 2017, **91**:46-58.
11. Xu J, Potter M, Tomas C, Elson JL, Morten KJ, Poulton J, Wang N, Jin H, Hou Z, Huang WE: **A new approach to find biomarkers in chronic fatigue syndrome/myalgic encephalomyelitis (CFS/ME) by single-cell Raman micro-spectroscopy**. *Analyst* 2019, **144**:913.
12. Krafft C, Schmitt M, Schie IW, Cialla-May D, Matthäus C, Bocklitz T, Popp J: **Label-free molecular imaging of biological cells and tissues by linear and nonlinear Raman spectroscopic approaches**. *Angew Chem* 2017, **56**:4392-4430.
13. Managó S, Migliaccio N, Terracciano M, Napolitano M, Martucci NM, De Stefano L, Rendina I, De Luca AC, Lamerti A, Rea I: **Internalization kinetics and cytoplasmic localization of functionalized diatomite nanoparticles in cancer cells by Raman imaging**. *J Biophotonics* 2018, **11**:e201700207.
14. Abalymov AA, Verkhovskii RA, Novoselova MV, Parakhonskiy BV, Gorin DA, Yashchenok AM, Sukhorukov GB: **Live-cell imaging by confocal Raman and fluorescence microscopy recognizes the crystal structure of calcium carbonate particles in HeLa cells**. *Biotechnol J* 2018, **13**:1800071.
15. Liao Z, Sinjab F, Elsheikha HM, Notinger I: **Optical sectioning in multifoci Raman hyperspectral imaging**. *J Raman Spec* 2018, **49**:1-8.
16. St-Arnaud K, Aubertin K, Strupler M, Madore WJ, Grosset AA, Petrecca K, Trudel D, Leblond F: **Development and characterization of a handheld hyperspectral Raman imaging probe system for molecular characterization of tissue on mesoscopic scales**. *Med Phys* 2018, **45**.
17. Hobro AJ, Smith NI: **An evaluation of fixation methods: spatial and compositional cellular changes observed by Raman imaging**. *Vib Spectrosc* 2017, **91**:31-45.
18. Pezzotti G, Horiguchi S, Boschetto F, Adachi T, Marin E, Zhu W, Yamamoto T, Kanamura N, Ohgitani E, Mazda O: **Raman imaging of individual membrane lipids and deoxynucleoside triphosphates in living neuronal cells during neurite outgrowth**. *ACS Chem Neurosci* 2018, **9**.
19. • Zhang S, Song Z, Godaliyadda GMDP, Ye DH, Chowdhury AU, Sengupta A, Buzzard GT, Bouman CA, Simpson GJ: **Dynamic sparse sampling for confocal Raman microscopy**. *Anal Chem* 2018, **90**:4461-4469.

The authors presented an algorithm using spectral feedback to dynamically sample measurement locations for Raman images. Coupled with a support vector machine (SVM) classifier, this allowed molecular images to be obtained with sixfold less measurements without sacrificing classification accuracy or spatial resolution.

20. Rowlands CJ, Varma S, Perkins W, Leach I, Williams H, Notingher I: **Rapid acquisition of Raman spectral maps through minimal sampling: applications in tissue imaging**. *J Biophotonics* 2012, **5**:220-229.
21. Kong K, Rowlands CJ, Elsheikha H, Notingher I: **Label-free molecular analysis of live *Neospora caninum* tachyzoites in host cells by selective scanning Raman micro-spectroscopy**. *Analyst* 2012, **137**:4119-4122.
22. Shipp DW, Rakha EA, Koloydenko AA, Macmillan RD, Ellis IO, Notingher I: **Intra-operative spectroscopic assessment of surgical margins during breast conserving surgery**. *Breast Cancer Res* 2018, **20**:69.
23. Boitor R, Kong K, Shipp D, Varma S, Koloydenko A, Kulkarni K, Elsheikh S, Bakker Schut T, Caspers P, Puppels G *et al.*: **Automated multimodal spectral histopathology for quantitative diagnosis of residual tumour during basal cell carcinoma surgery**. *Biomed Opt Exp* 2017, **8**:5749-5766.
24. • Corden CJ, Shipp DW, Matousek P, Notingher I: **Fast Raman spectral mapping of highly fluorescing samples by time-gated spectral multiplexed detection**. *Opt Lett* 2018, **43**:5733-5736.

Combining the speed and sensitivity of a single photon avalanche photodiode (SPAD), the chemical specificity of a Raman spectrometer, and the dynamic selectivity of a digital micromirror device (DMD), the authors presented the first images acquired by time-gates Raman spectroscopy. This technique allowed molecular images in dyed samples where the fluorescence noise normally overwhelms the weaker Raman signal.

25. Wang Y, Huang WE, Cui L, Wagner M: **Single cell stable isotope probing in microbiology using Raman microspectroscopy**. *Curr Opin Biotech* 2016, **41**:34-42.
26. Naemat A, Sinjab F, McDonald A, Downes A, Elfick A, Elsheikha HM, Notingher I: **Visualizing the interaction of *Acanthamoeba castellanii* with human retinal epithelial cells by spontaneous Raman and CARS imaging**. *J Raman Spectrosc* 2018, **49**:412-423.
27. Li S, Chen T, Wang Y, Liu L, Lv F, Li Z, Huang Y, Schanze KS, Wang S: **Conjugated polymer with intrinsic alkyne units for**

synergistically enhanced Raman imaging in living cells. *Angew Chem* 2017, **129**:13640-13643.

28. Ramoji A, Galler K, Glaser U, Henkel T, Mayer G, Dellith J, Bauer M, Popp J, Neugebauer U: **Characterization of different substrates for Raman spectroscopic imaging of eukaryotic cells**. *J Raman Spectrosc* 2016, **47**:773-786.

29. • Sinjab F, Sicilia G, Shipp DW, Marlow M, Notingher I: **Label-free Raman hyperspectral imaging of single cells cultured on polymer substrates**. *Appl Spectrosc* 2017, **71**:2595-2607.
The authors acquired Raman images of cells despite the cells being cultured on a polymer substrate. Polymer substrates are commonly used in pharmacology and biomaterial research. The strong Raman signature of polymers had prohibited measurements under such conditions before this work.

30. Lieber CA, Mahadevan-Jansen A: **Automated method for subtraction of fluorescence from biological Raman spectra**. *Appl Spectrosc* 2003, **57**:1363-1367.

31. Prats-Mateu B, Felhofer M, de Juan A, Gierlinger N: **Multivariate unmixing approaches on Raman images of plant cell walls: new insights or overinterpretation of results?** *Plant Methods* 2018, **14**:52.

32. Byrne HJ, Knief P, Keating ME, Bonnier F: **Spectra pre and post processing for infrared and Raman spectroscopy of biological tissues and cells**. *Chem Soc Rev* 2016, **45**:1865-1878.

33. Kochan K, Peng H, Gwee ESH, Izgorodina E, Haritos V, Wood BR: **Raman spectroscopy as a tool for tracking cyclopropane fatty acids in genetically engineered *Sccharomyces cerevisiae***. *Analyst* 2019, **144**:901.

34. Yildirim T, Matthaeus C, Press AT, Schubert S, Bauer M, Popp J, Schubert US: **Uptake of retinoic acid-modified PMMA nanoparticles in LX-2 and liver tissue by Raman imaging and intravital microscopy**. *Macromol Biosci* 2017, **17** 1700064.

35. Musto P, Calarco A, Pannico M, LaManna P, Margarucci S, Tafuri A, Peluso G: **Hyperspectral Raman imaging of human prostatic cells: an attempt to differentiate normal and malignant cell lines by univariate and multivariate data analysis**. *Spectrochim Acta Part A Mol Biomol Spectrosc* 2017, **173**:476-488.

36. •• Kallepitis C, Bergholt MS, Mazo MM, Leonardo V, Skaalure SC, Maynard SA, Stevens MM: **Quantitative volumetric Raman imaging of three dimensional cell cultures**. *Nat Commun* 2017, **8**:14843.
In this ambitious study, the authors acquired Raman hyperspectral images in three dimensions. Three dimensional images were acquired as stacks of two-dimensional images, using vertex component analysis (VCA) to display images of pure chemical components.